



Thymoquinone Nanoparticles (TQ-NPs) in Kidney Toxicity Induced by Ehrlich Ascites Carcinoma (EAC): An In Vivo Study

Canadian Journal of Kidney Health and Disease
Volume 11: 1–9
© The Author(s) 2024
Article reuse guidelines:
sagepub.com/journals-permissions
DOI: 10.1177/20543581241258812
journals.sagepub.com/home/cjk



Zakaria Eltahir^{1,2} , Maha Ibrahim³,
Muniera Y. Mohieldeen⁴, Ammar Bayoumi³,
and Samia M. Ahmed⁵

Abstract

Background: Cisplatin (Cis) is potent chemotherapy used to treating already many different types of cancer; however, it is found to correlate with nephrotoxicity and other adverse health consequences. Thymoquinone (TQ) is an antioxidant and anti-inflammatory molecule that may defend against the consequences of different chemotherapies. Thymoquinone uses, although, are negatively impacted by its weak solubility and inadequate biological availability.

Objectives: This investigation examined the efficacy of a new nanoparticle (NP) absorbing TQ in an Ehrlich Ascites Carcinoma (EAC) mice model to address its low solubility, enhance its bioavailability, and protect against Cis-induced nephrotoxicity.

Methods: Following 4 treatment groups were included in this research: (1) control, (2) EAC, (3) EAC + Cis + Thymoquinone nanoparticle (TQ-NP) treated, and (4) EAC + Cis-treated.

Results: The study revealed that TQ-NP was efficacious in avoiding Cis-induced kidney problems in EAC mice, as well as restoring kidney function and pathology. Thymoquinone nanoparticle considerably reduced Cis-induced oxidative damage in renal tissue by augmenting antioxidant levels. According to tumor weight and histological investigation results, TQ-NP did not impair Cis's anticancer efficacy.

Conclusion: Thymoquinone nanoparticle might be used as a potential drug along with Cis anticancer therapy to reduce nephrotoxicity and other side effects while maintaining Cis anticancer properties.

Abrege

Contexte: Le cisplatine (CIS) est un puissant agent chimiothérapeutique utilisé pour le traitement de nombreux types de cancers. Le cisplatine est cependant corrélé à de la néphrotoxicité et à d'autres conséquences néfastes pour la santé. La thymoquinone (TQ) est une molécule antioxydante et anti-inflammatoire qui peut protéger contre les effets néfastes de différents agents chimiothérapeutiques. Les faibles solubilité et biodisponibilité de la TQ limitent toutefois son utilisation.

Objectifs: Un modèle de souris atteintes d'un carcinome ascitique d'Ehrlich (souris EAC) a servi à vérifier l'efficacité d'une nouvelle nanoparticule (NP) absorbant la TQ pour remédier aux faibles solubilité et biodisponibilité de la TQ et protéger contre la néphrotoxicité induite par le CIS.

Méthodologie: Les quatre groupes suivants ont été examinés: i) témoin; ii) souris EAC; iii) souris EAC traitées par CIS + TQ-NP (thymoquinone-nanoparticule); iv) souris EAC traitées par CIS.

Résultats: L'étude a révélé que la TQ-NP était efficace pour éviter les problèmes rénaux induits par le CIS chez les souris EAC, de même que pour restaurer la fonction rénale et soigner la pathologie. En augmentant les niveaux d'antioxydants, la TQ-NP a considérablement réduit les dommages oxydatifs induits par le CIS dans le tissu rénal. Selon le poids des tumeurs et les résultats de l'étude histologique, la TQ-NP n'a pas altéré l'efficacité anticancéreuse du CIS.

Conclusion: La TQ-NP pourrait potentiellement être utilisée avec le traitement anticancéreux par CIS afin de réduire la néphrotoxicité et les autres effets secondaires, sans altérer les propriétés anticancer du CIS.

Keywords

thymoquinone, kidney toxicity, Ehrlich ascites carcinoma, cisplatin, cancer treatment

Received February 15, 2023. Accepted for publication May 6, 2024.



Introduction

Cancers of many different sorts are treated with cisplatin (Cis). Based on its propensity to induce deoxyribonucleic acid (DNA) and trigger cytotoxic DNA damage, Cis can annihilate cancer cells.¹ However, it generates apoptosis and diminishes the effectiveness of cell healing.² Myelosuppression, nausea, and vomiting are among the unfavorable side effects of Cis use.³ Rapid deterioration in the kidney function is considered to be a significant deleterious reaction of using Cis as well.⁴ In laboratory animals, the first nephron segment after the glomerulus is primarily seriously affected by Cis.⁵ The notable histopathological hallmarks of Cis-induced nephrotoxicity in animal research include extensive necrosis and progressive degeneration of renal proximal tubular epithelial cells.⁶ The underlying mechanism by which Cis-induced nephrotoxicity caused is heavily contested. Numerous processes, including apoptosis, free radicals, inflammation, and hypoxia, have been postulated.⁷

When used with traditional remedy, complementary therapy can produce excellent outcomes with fewer side effects and improved therapeutic resistance. Black cumin or black seed, also known as thymoquinone (TQ), a monoterpene, is the predominant effective component of *Nigella sativa*.⁸ It contains antiphlogistic and antioxidizing qualities and can prevent a variety of malignant cancers.⁹ Thymoquinone has been shown to decrease leukemia cell proliferation and induce apoptosis.¹⁰⁻¹² Several studies have found that a high dosage of TQ exacerbated the nephrotoxic harmful effects of Cis in cancer-free female rats.¹³ On the contrary, numerous different studies have concluded that minimal concentrations of TQ protect rats against Cis-induced nephrotoxicity.¹³⁻¹⁷ Another recently published research study found that combining TQ with curcumin at high doses protects against Cis-induced nephrotoxicity.¹⁸ Thymoquinone-chemotherapeutics amalgamation boosted the antitumor effect of numerous chemotherapeutic drugs while mitigating their harmful effects on normal cells and tissues due to their antioxidant properties.¹⁹ The disadvantages of using TQ as a primary pharmaceutical drug are connected to its low solubility, which impairs its bioavailability.^{20,21}

The Ehrlich carcinoma model is widely used in cancer research as it easily grows in the peritoneal cavity. It has also, shown to proliferate and metastases violently in the absence of the estrogen hormone.²² Thus, this study elected to focus specifically on male mice for better outcomes to achieving the aims of the study. The planned study would assess the potential protective advantages of TQ.

Thymoquinone nanoparticles (TQ-NPs) research plans to work on TQ's restorative characteristics, like its targeting specificity, bioavailability, and potential for unspecific binding. Thymoquinone nanoparticles surpassed free TQ in studies considering different TQ-NPs compositions in contrast to renal harm and cancer.²³ Niosomal, liposomal, polymeric, solid lipid nanocarriers (SLNs), and nanostructured lipid

carriers (NLCs) were contained in these formulations.²⁴ Thymoquinone is a potential anticancer medication that smother cancer cell development and its progression in vitro experimental animal model. Also, using of NP formulation against Ehrlich Ascites Carcinoma (EAC) might lead to renal failure in male mice.²⁵ Regardless of TQ's huge pharmacological properties, its clinical interpretation is hampered by its narrow therapeutic index and hydrophobicity.²⁵ Accordingly, we and others implanted TQ in NPs to increase efficiency and limit anticancer activity. When these TQ-NP formulations were equated to Cis, a chemotherapeutic therapy used to treat kidney cancer, the former had predominant anticancer and mitigating properties.²⁴⁻²⁶ We give a depiction of the numerous TQ-NP formulations, underline their unprecedented efficiency, and examine conventional procedures to help TQ bioavailability and anticancer movement, expanding the chance of clinical therapy.

Materials and Methods

Protocols

Initially, Swiss albino healthy male mice of 8 weeks age and 25 g body weight, were either injected with saline or the Ehrlich tumor cells (1×10^4 - 10^7 in 25 μ L) intraplantar (i.pl.). Between 0 and 12 days, assessments of paw edema/tumor development, mechanical and thermal hyperalgesia, and overt pain-like behavior were recorded. The dose of 1×10^6 /paw of tumor cells was determined for the subsequent studies of mechanical and thermal hyperalgesia, paw edema/tumor development, and histological examination at the designated time points based on the results. For tests involving overt discomfort, 1×10^7 tumor cells/paw and assessment on day 8 following inoculation were selected. After 12 days of tumor injection, paw specimens were collected for histological and microscopic examinations. To determine the hyperalgesic action of cellular fragments, Ehrlich tumor cells were inactivated and administered i.pl., then compared to saline and active Ehrlich tumor cell groups. The computations were

¹Department of Clinical Laboratory Sciences, Faculty of Applied Medical Science, Taibah University, Medina, Saudi Arabia

²Research Unit, School of Medicine, Taibah University, Medina, Saudi Arabia

³MSF Medical Scientific Foundation for Research & Development, King Abdulaziz University, Jeddah, Saudi Arabia

⁴Department of Biochemistry, College of Medicine, King Khalid University, Abha, Saudi Arabia

⁵Clinical Biochemistry, Department of Clinical Laboratory Sciences, Faculty of Applied Medical Science, Taibah University, Medina, Saudi Arabia

Corresponding Author:

Zakaria Elthahir, Associate Professor in Histopathology and Molecular Oncology, Department of Clinical Laboratory Sciences, Faculty of Applied Medical Science, Taibah University, Medina, Saudi Arabia.
Email: Zidrees@taibahu.edu.sa

measured on days 0 to 12. To assess the pharmacological modulation of Ehrlich tumor-induced pain-like behavior, mice were treated with Cis (5 mg/kg) i.pl. injection and TQ-NP treatment was given orally with a dosage of 10 mg/kg on the eighth day after Ehrlich tumor cells treatment, and quantifying paw edema/tumor growth and mechanical and thermal hyperalgesia.

Thymoquinone Nanoparticles

Thymoquinone nanoparticles were prepared with poly lactic-co-glycolic acid (PLGA) using the solid/oil/water (S/O/W) solvent evaporation method as previously described.²⁶ An optimized TQ-NP formulation in the form of oil-filled nanocapsules (F2-NC) was obtained with a mean hydrodynamic diameter of 117 nm, (polydispersity index) PDI of 0.16, about 60% loading efficiency, and sustained in vitro drug release. Briefly, PLGA (Sigma, St. Louis, Missouri) was dissolved in high-performance liquid chromatography (HPLC)-grade dichloromethane (DCM) as an oil phase for 12 hours to obtain uniform solution followed by the addition 5 mg TQ. The suspension was sonicated for 2 minutes to generate S/O primary emulsion that was emulsified with an aqueous phase of 20 mL saline with polyvinyl alcohol (1%) to form S/O/W emulsion using a magnetic stirrer for about 7 rcf. The mixture was vortexed for 10 seconds at a high setting followed by ultrasonication (20 KH2) for 3 minutes to generate the final S/O/W emulsion. The organic solvent was evaporated using a rotary evaporator at 50°C. Following centrifugation for about 9000 rcf for 20 minutes at 4°C, the synthesized material was collected and resuspended in 2% sucrose. The shape and size of the particles were confirmed using transmission electron microscope (TEM) (TEM is described in details in the literature^{27,28}). The suspension of TQ-PLGA NPs exhibited turbid white color, and the NPs were spherical in shape and 20 nm (10-30 nm) sized with 80% encapsulation efficiency. Nanoparticles suspension was subjected to centrifugation for about 80000 rcf for 15 minutes. The supernatant was removed, and 1 mL of methanol was added to the sediment which was treated with sonication for 5 minutes and then injected to HPLC to measure the amount of TQ.²⁹⁻³¹ The EE was 80% as calculated using the following equation:

$$EE\% = \text{Total TQ-nanoencapsulated TQ} / \text{total TQ} \times 100$$

Cell Line Tested and Authenticated [from the source]

The non-human cell line identification is used. Mouse cell line authentication method was adopted to test cells. A multiplex polymerase chain reaction assay targeting 9 tetranucleotides short tandem repeat (STR) markers in the mouse genome. Mouse cell line authentication test in India is the

most common model system and we perform STR profiling following ISO9001 and ISO/IEC17025 quality standards. Short tandem repeat for validated mouse cell lines at 18 STR markers. Consensus allele calls (greater than 98%). Primers were used to sequence STR regions to determine actual number of repeats (alleles) and correlate with fragment length obtained using capillary electrophoresis.

Mouse multiplex polymerase chain reaction (PCR) assay is as follows:

- Forward Primer (5'-3')
- TCTTTCTCCTTTTGTGTCATGC
- Reverse Primer (5'-3')
- GTTTCTTGCTAAATAACTAAGCAAGTGAACAGA

Cell Line Preparation Before Inoculation

Ehrlich's Ascites Carcinoma (EAC) cell lines were received since 2/2021. Cells were tested at 3/2021 and then we immediately used them in experimental models. Cells were provided by the Indian Institute of Chemical Biology (IICB), Kolkata, India (EAC strain 7 transplantable mouse carcinoma sources). The IICB followed UKCCCR Guidelines for the Use of Cell Lines in Cancer Research.³² To check the in vitro cell viability before inoculation into the experimental mice groups we applied MTT assay (MTT Assay Kit MyBiosource Catalog No: MBS2540588). The MTT cell viability measurements protocol for tumor growth was conducted according to standard manufacturers' description. To observe the EAC cells, the ascitic fluid obtained from treated mice was stained with DAPI fluorescent dye and kept in dark condition at 37°C for 15 minutes, and then to measure cellular metabolic activity as an indicator of cell viability, proliferation, and cytotoxicity readings absorbance at 570 nm. Protocol was applied once before the inoculation of cancer cells to ensure cell lines are adequate for the planned mice experiments (Figure 1).

The Ehrlich Tumor Cells Inoculation

Ten days following the introduction of the tumor, Ehrlich tumor cells were taken from the ascitic fluid in the peritoneal cavity of mice. The ascitic fluid was 3 times rinsed with phosphate-buffered saline (PBS), pH 7.4, subjected to centrifugation (200 g, 10 minutes), and rinsed 3 times with PBS. The Neubauer chamber was used to test the cell viability using the 0.5% trypan blue exclusion method, steps were applied according to the Trypan Blue Exclusion Method as previously described.³³ In 25 μ L of saline, the Ehrlich tumor cells were diluted to final concentrations of 1×10^4 , 1×10^5 , 1×10^6 , and 1×10^7 . Measurements were conducted before and following the injection of cancer cells on days 0 through 12.

Table 1. Animal Grouping and Experimental Design.

Group		Experimental design		
		Preinoculation (1st–15th day)	Inoculation day 0	Postinoculation 3 days after
G1	Control	Distilled water every day orally		
G2	EAC	-	0.2 mL of 2.5×10^6 EAC cells/mice, i.p	-
G3	TQ-NP + Cis-treated	Distilled water every day orally		TQ-NP (100 mg/kg) orally every day + Cis (5 mg/kg), i.p everyday
G4	Cis-treated only	Distilled water every day orally		Cis (5 mg/kg), i.p everyday

Experimental Design

Forty Swiss albino male mice, 8 weeks adults, body weight 25 g supplied from animal holding facility, within the university pharmacy veterinary laboratory, were acclimatized, and divided into 4 groups, 10 mice in each group (Table 1). The assessment of blood biomarkers for the renal function test of urea and creatinine to evaluate kidney oxidative damage as reflected in glutathione (GSH) level, and furthermore, tumor growth and inflammation impact was also assessed by measuring the tumor necrosis factor (TNF- α) levels. At the end of experiments and before mice scarification and biopsied for histological analysis, serum samples were obtained from across the experimental mice groups. 1.0 mL of whole blood collected and allowed to clot, then centrifuged for about 90 rcf for 10 minutes to separate the serum to be stored at -20°C until biochemical tests performed.

Control group (G1): This group of mice was given distilled water every day orally till the last day of the experiment.

EAC group (G2): On the day “0,” the EAC group was injected intraperitoneally (i.p) 0.2 mL of 2.5×10^6 EAC cells/mouse.³⁴

Cis + TQ-NP treated (Cis and TQ-NP) group (G3): Distilled water was given orally to mice every day for 2 weeks before and 3 days after EAC injecting. A single dose of Cis (5 mg/kg), i.p./daily (till the end of the experiment), and a TQ-NP (100 mg/kg) dose were administered orally every day till the end of the experiment.

Cis-treated group (G4): This group was administered distilled water in the same way as the previous group; the mice were then treated with a single dose of Cis (5 mg/kg), i.p every day till the end of the experiment.³⁵

Statistical Analysis

Data analysis was done by using SPSS (version 26.0; SPSS Inc, Chicago, Illinois) for Microsoft Windows. Results were calculated as mean \pm standard deviation (SD) and the group variables were given as numbers and percentages (%). An unpaired *t*-test was used for comparing 2 means, whereas

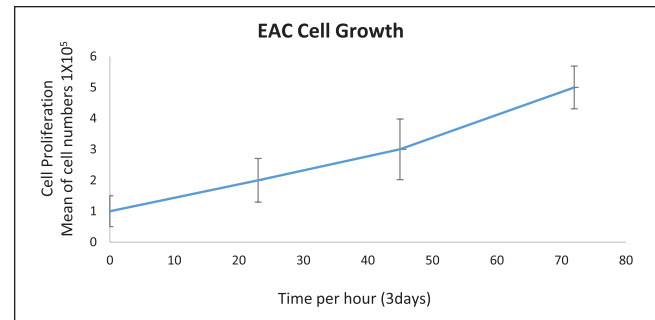


Figure 1. Initial evaluation of in vitro cell viability, this has been measured to determine cell line viability and tumor growth rate prior to the inoculation of the EAC into the planned 40 mice experimental animals.

chi-square was achieved for comparing the frequency of 2 groups or more. The strength of a relationship between 2 variables was evaluated using the Pearson’s correlation test. $P < .05$ is the measure of significance. Each value represents the mean \pm SEM (standard error of the mean) of the group using 1-way analysis of variance (ANOVA) test.

Histological Preparation and Interpretation

Experimental mice were sacrificed and both kidneys from across the experimental mice were biopsied and fixed in 10% neutral buffered formalin solution and then samples were processed into a paraffin wax blocks, a 4 μm thick paraffin sections were obtained. The sections were stained for histological hematoxylin and eosin (H&E) to observe and report pathological changes throughout the experimental mice. Anonymously and blindly histopathological analysis has been conducted across all samples and in a systematic fashion. The findings were reported blindly regardless of treatment group by experienced pathologist and later reports identified and compared to mice groups. After each mice group and the relevant treatment exposure was confirmed, findings were correlated to their specific groups, a representative histology for each of the 4 mice experimental groups was selected and shown in Figure 2.

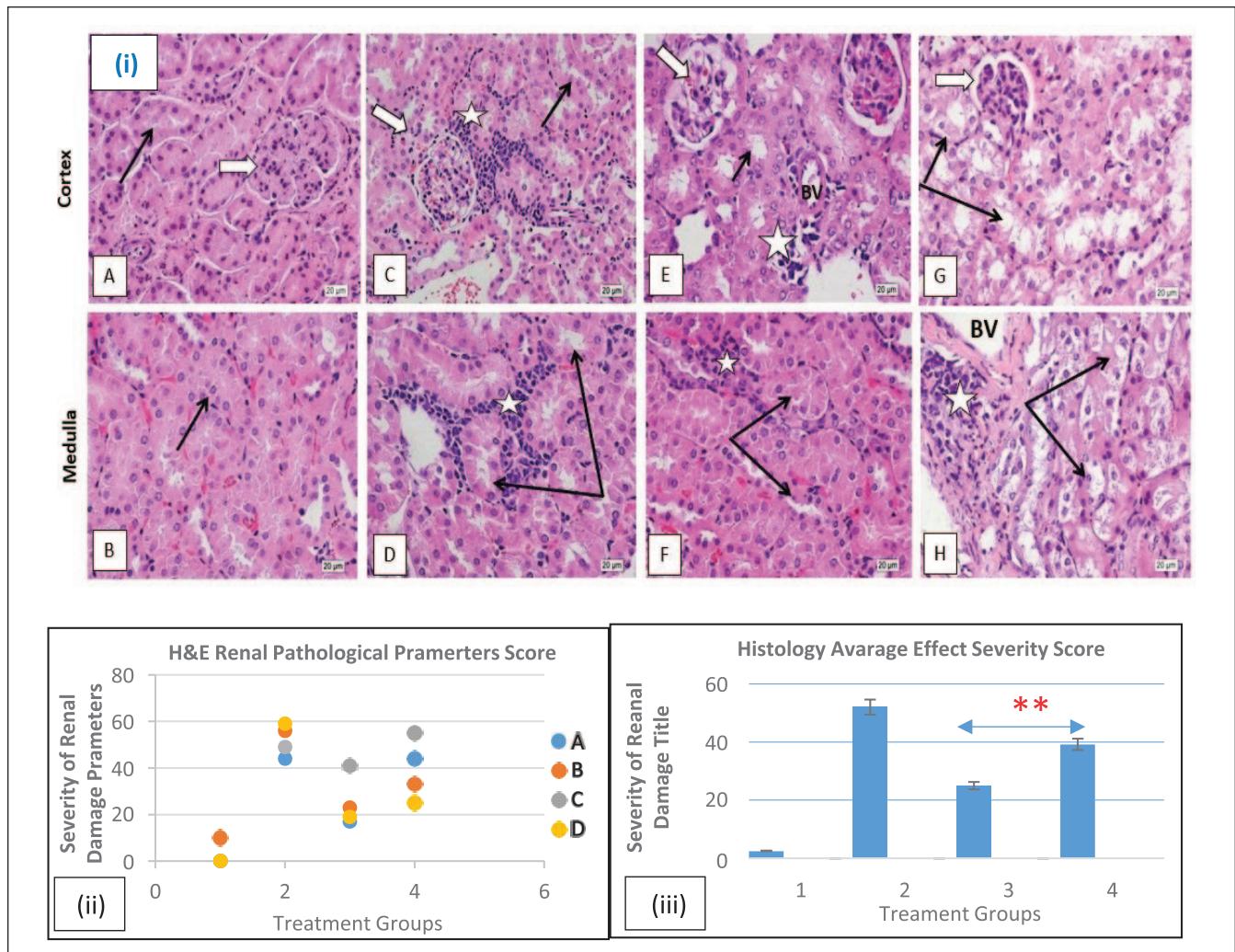


Figure 2. Histology study experimental design of 40 mice treated in 4 different groups. Shown here are the representative micrographs of H&E-stained histology sections (4 μ m) (magnification: $\times 40$) mice kidney cortex and medulla to show renal corpuscles (white arrows) glomerular capillaries (black star), kidney tubules (black arrows) and neoplastic cells (white star) histological analysis revealed: **Control (G1)** (A and B): shows normal renal corpuscle and glomerular capillaries. Kidney cortical and medullary tubules showed normal narrow lumina and lining epithelium. **Ehrlich group (G2)** (C and D): aggregations of infiltrating viable neoplastic cells mild decrease in renal corpuscle and glomerular size also dilation of tubular lumina were seen. **Ehrlich + Cis + TQ-NP (G3)** (E and F): showing marked preservation of kidney parenchyma structure against Cis toxicity and slight deformity of some renal corpuscles. Kidney tubules showed healthy lining epithelium similar to that of control with slight luminal dilation in the cortical region. Neoplastic cells near blood vessels showed also features of degenerative involution as also seen dark pyknotic nuclei (apoptosis). **Ehrlich + Cis (G4)** (G and H): shows marked disorganization of renal parenchyma with deformity, atrophy of renal corpuscle, and glomeruli. Kidney tubule lining epithelium showed marked degenerative hydropic changes (swollen cells, unstained cytoplasm, and deformed small nuclei). Neoplastic cells near blood vessels (BVs) looked unviable and degenerated, dark pyknotic nuclei (apoptosis). **(i) and (ii)** H&E-stained histologies scoring to assess renal effect severity parameters in morphological toxicity hall marks for the Ehrlich + Cis + TQ-NP in group 3 mice (G3) treatment has shown a significant morphological preservation to normal histology in comparison to Ehrlich + Cis treatment alone in group 4 (G4) as the current therapy model in practice, Fisher's exact test statistical analysis revealed (P-value was .01). The pathological hall mark parameters analyzed as follows: **A:** glomerular atrophy, **B:** glomerular capillaries deformities, **C:** dilatation of luminal tubules, **D:** neoplastic cell aggregations.

Furthermore, histopathological quantitative analysis was applied to establish average scores and semi-quantitative assessment applied to identify more subtle differences in kidney injury and to strengthen our previous reported

pathological findings. Each mice group (of 10) average score was calculated and analyzed to quantitatively assess the degree of severity for the histological/morphological changes in each treatment group of the mice. A previously

described semi-quantitative method for severity of histological/pathological scoring was used with minor modifications.^{36,37} The severity scores are often recorded using scale of [0-3], with [0] indicating no pathological effect or semi normal histological morphology, [1] indicating minimal pathological effect or morphological change, [2] moderate pathological effect, and [3] for severe effect. Fisher's exact test was applied to compare between the 2 groups in question: treatment in combination with QT-NP and without QT-NP.

Results

Histological Results

Group 1-Control (A and E): Displaying healthy renal corpuscles and glomerular capillaries (white arrow). Normal thin lumina and lining epithelium were also detected in the kidney cortical and medullary tubules (black arrows) (Figure 2).

Group 2-EAC (B and F): Exhibiting infiltrating viable neoplastic cell aggregation (white star), a slight reduction in renal corpuscle (white arrow) and glomerular (black star) size (white arrow), and tubular lumina dilatation (black arrows) (Figure 2).

Group 3-Ehrlich + Cis + TQ (D and H): Demonstrating significant preservation of kidney parenchyma structure against Cis poisoning, minor deformation of certain renal corpuscles (white arrow), kidney tubules revealed stable lining epithelium similar to control with mild luminal dilatation in the cortical area (black arrows). Degenerative involution was also seen in neoplastic cells surrounding blood arteries (white star) (Figure 2).

Group 4-Ehrlich + Cis (C and G): The renal parenchyma is fragmented, with deformity and degeneration of the renal corpuscle (white arrow) and glomeruli (black star). Degenerative hydropic alterations (swollen cells, unstained cytoplasm, and deformed small nuclei) were noticed in the kidney tubule lining epithelium (black arrows). Near blood vessels (BV), neoplastic cells (white star) seemed unviable and damaged (dark pyknotic nuclei) (Figure 2).

Final representative histology of induced leg solid Ehrlich carcinoma in a mice model were found to be transformed into aggressive infiltrating cells with highly characteristic pleomorphic nuclei associated with numerous mitotic figures. It massively infiltrated the underlying leg muscles and was found to metastasize to distant organs including the kidney, often via blood circulation, where it continues to proliferate near large BVs, and peritubular capillaries and tissues around. A single administration of Cis was found to moderately decrease the size of the growing tumor based on measuring mice leg weight and histologically findings of a decreasing the frequency of the presence of neoplastic cells

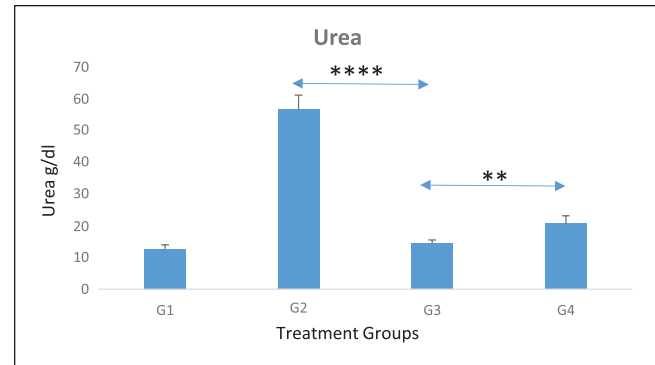


Figure 3. Graph shows average serum urea levels for experimental groups (each of 10 mice). Noticeable increased levels in most affected nephrotoxicity in untreated group (G2) by neither therapies Cis nor Cis + TQ-NP), whereas the nephrotoxicity was significantly decreased in those treated with combined (Cis + TQ-NP) therapy (G3), when compared with untreated group (G2) ($P = .0000117$). Also, when comparing between Cis and Cis + TQ-NP groups (G4 and G3), nephrotoxicity was significantly decreased, this was shown in urea biochemical level, results were lower than Cis only treated group (G4) ($P = .01$).

deep in kidney tissue and their deformative appearance. However, Cis nephrotoxicity was observed in the kidneys of treated mice (Figure 2).

Discussion

The ongoing research demonstrated that renal function was impaired in EAC-bearing mice, as exemplified by higher serum urea and creatinine levels (Figures 3 and 4). In addition to these observations, different vascular, degenerative, and inflammatory pathological alterations were detected in the renal tissue of EAC-bearing mice, as well as a substantial infiltration of neoplastic cells. Abd Eldaim et al,³⁸ Donia et al,³⁹ and Hashem et al⁴⁰ are in agreement with these findings. Following that, the increase in kidney functional biomarkers could be compared to renal damage sustained by tumor metastasis and cancerous cells infiltration in renal tissue. Thus, resulting in abnormal proximal tubules reabsorption and glomerular filtration rate, plus a decrease in urea and creatinine excretion, contributing to higher blood levels.⁴¹ A significant evaluated renal function test urea and creatinine recorded kidney oxidative damage as demonstrated by substantial decreases in the reduced GSH. A precursor for tumor progression that ultimately decreases the cellular antioxidants and, subsequently, induces renal tissue damage. Oxidative stress is well known to be one of the most contributing factors to cancer initiation and progression. It is also implicated as a potential mechanism of EAC-induced renal damage.⁴⁰ On the contrary, mice groups (G3 and G4) have been treated with Cis chemotherapy similarly. Thus, in fact, it would also impact these histological findings.^{4,6,42-44} Certainly, treatment was equally introduced onto both

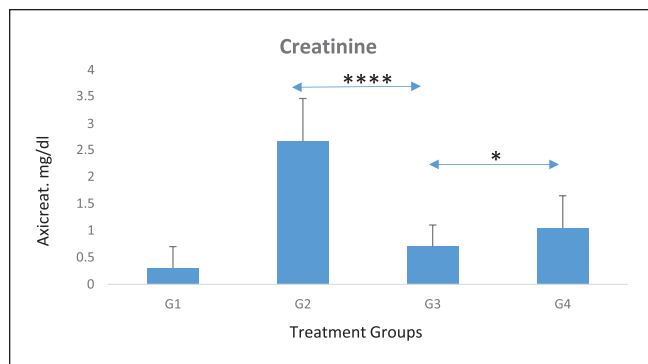


Figure 4. Graph shows average serum creatinine levels for each experimental group (of 10 mice). Noticeably increased creatinine levels in most affected nephrotoxicity untreated group (G2) and significantly decreased in those treated with combined (Cis + TQ-NP) therapy (G3) ($P = .00005$). When comparing between Cis and Cis + TQ-NP groups (G4 and G3), nephrotoxicity was significantly decreased, this was represented in creatinine biochemical level, results were slightly lower than Cis only treated group (G4) ($P = .03$). The differences between (G1 and G3) and (G1 and G4) groups were noted; certainly, this is reflecting the none-fully restoration of kidneys functionality at this point of experimental window timeline, but a great significant restoration was reported as above and confirmed later in histology (Figure 2).

groups, therefore, this does not exclude the impact of this well-known aggressive chemotherapy implications on histological changes; however, this study was not aiming to study this indicator as far as to soften and minimize the severity of histological damage that caused by either EAC or Cis treatment by applying TQ-NP (G3) and compare the findings with the current approach in clinical practice of today (G4).

Effect of TQ-NP on Ehrlich tumor induced tumor and inflammation impact on serum TNF- α levels in experimental mice. Statistical analysis when comparing the EAC tumor in untreated with Cis nor QT-NP group (G2) with the third experimental group (G3) (Cis + TQ-NP) dose treated shows a significantly decreased TNF- α levels ($P \leq .0007$). Also, analysis shows a significant increase in glutathione (GSH) levels ($P \leq .00001$). However, there was no significance differences in TNF- α and GSH between the Cis only treatment and Cis combined TQ-NP treatment groups (G3 vs G4) ($P = .09$ vs $P = .06$, respectively) (Figures 5 and 6). Interestingly, previous research also found some of the renal biochemical markers have no significant differences in a related nephrotoxicity study in brown Norway rats, as in Cis-treated mice in developing a new platform for early detection in nephrotoxicity and in acute nephrotoxicity.⁴²⁻⁴⁴

Conclusion

This study has revealed the combination of TQ-NP and cisplatin therapy could play a role in future innocuous

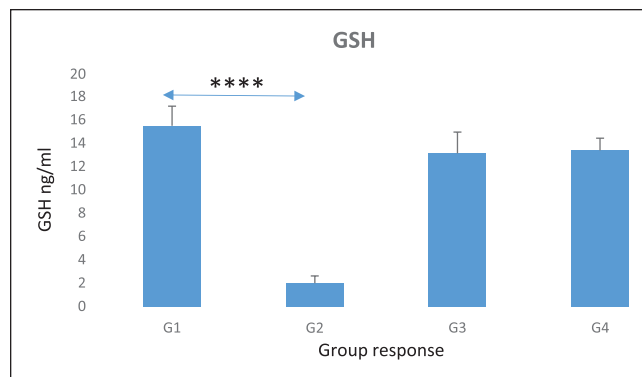


Figure 5. This graph shows GSH antioxidant factor across the 4 mice experiments groups (total of 40 mice studied). A significant negative correlation between the (Cis + TQ-NP) of 10 mice treated (G3) group, and the EAC tumor 10 mice (G2) group ($P \leq .00001109$), this confirming a significant decreased GSH levels in the (10 mice) group (G2) untreated. However, there was no significant difference in GSH levels between G3 and G4 groups ($P = .06$).

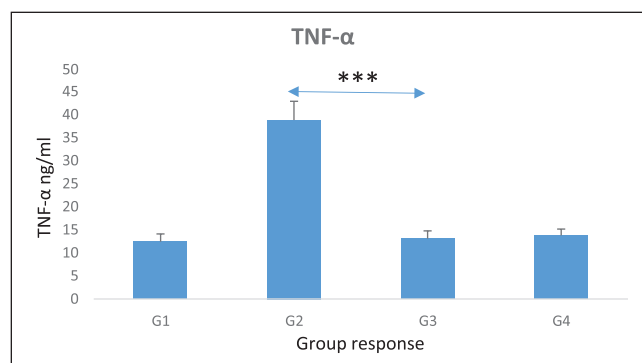


Figure 6. This graph shows TNF- α levels across the 4 mice experimental groups (total of 40 mice). The correlation between the (Cis + TQ-NP) treated 10 mice group (G3) and the EAC tumor group (G2) was statistically significant ($P \leq .0007$), while slight but not significant TNF- α increase in G4 than G3; however, the effect of the TQ-NP on induced nephrotoxicity in experimental mice was significantly decreased. However, there was no significant difference in TNF- α levels between G3 and G4 groups ($P = .09$).

cancer treatment design. Histological observations and histology quantitative analysis both have shown significantly a marked preserved normal kidney's parenchyma and tubular morphology without interfering with the cisplatin drug bioactivity in defeating cancer cells. Levels of blood creatinine and urea biomarkers were significantly decreased reflecting healthier kidney function. Further studies are needed to investigate the mechanism of how TQ-NP would minimize the nephrotoxicity implication on kidneys.

Acknowledgments

The authors are thankful to their universities for the continuous support of this study.

Author Contributions

All authors are responsible for the concept and design of the study. Z.E., M.I., A.B., and S.A. contributed to data acquisition. A.B., M.Y.M., Z.E., and S.A. contributed to data analysis. Z.E. and M.I. interpreted the results and drafted the manuscript. All authors contributed to the creation, critically revised, and approved the manuscript final version to be published, and agreed to be accountable for all aspects of the work.

Declaration of Conflicting Interests

The author(s) declared no potential conflicts of interest with respect to the research, authorship, and/or publication of this article.

Funding

The author(s) received no financial support for the research, authorship, and/or publication of this article.

Consent for Publication

The authors agree to the final version of the paper.

Ethical Approval and Consent to Participate

Protocols for animal experiments were approved by the Animal Experimental Ethics Committee of the King Abdulaziz University (approval no. p745-2020), in compliance with the Saudi Law of Ethics of Research on Living Creatures guidelines for the care and use of laboratory animals. Methods were performed according to the recommendations of Good Clinical Practice and the Declaration of Helsinki (2013).

Consent for Publication

Not applicable.

Availability of Data and Materials

All relevant data are included in this published article.

ORCID iD

Zakaria Eltahir  <https://orcid.org/0000-0001-6815-4100>

References

- Siddik ZH. Cisplatin: mode of cytotoxic action and molecular basis of resistance. *Oncogene*. 2003;47:7265-7279.
- Desoize B, Madoulet C. Particular aspects of platinum compounds used at present in cancer treatment. *Critical Rev Oncol Hematol*. 2002;42:317-325.
- Tsang RY, Al-Fayea T, Au H-J. Cisplatin overdose. *Drug Safety*. 2009;32: 1109-1122.
- Miller RP, Tadagavadi RK, Ramesh G, Reeves WB. Mechanisms of cisplatin nephrotoxicity. *Toxins*. 2010;2:2490-2518.
- Leibbrandt ME, Wolfgang GH, Metz AL, Ozobia AA, Haskins JR. Critical subcellular targets of cisplatin and related platinum analogs in rat renal proximal tubule cells. *Kidney Int*. 1995;48(3):761-770.
- Dobyan DC, Levi J, Jacobs C, et al. Mechanism of cis-platinum nephrotoxicity: II. Morphologic observations. *J Pharmacol Exp Therapeut*. 1980;213:551-556.
- Uehara T, Yamate J, Torii M, Maruyama T. Comparative nephrotoxicity of cisplatin and nedaplatin: mechanisms and histopathological characteristics. *J Toxicol Pathol*. 2011;24(2):87-94.
- Hajhashemi V, Ghannadi A, Jafarabadi H. Black cumin seed essential oil, as a potent analgesic and antiinflammatory drug. *Phytotherap Res*. 2004;18:195-199.
- Wanner M, Koomen G, Dung NX, Thymoquinone from Eupatorium ayapana. *Planta Medica*. 1993;59:99.
- Shoieb AM, Elgayyar M, Dudrick PS, Bell JL, Tithof PK. In vitro inhibition of growth and induction of apoptosis in cancer cell lines by thymoquinone. *Int J Oncol*. 2003;22(1): 107-113.
- Harakeh S, Abu-El-Ardat K, Diab-Assaf M, Niedzwiecki A, El-Sabban M, Rath M. Epigallocatechin-3-gallate induces apoptosis and cell cycle arrest in HTLV-1-positive and-negative leukemia cells. *Med Oncol*. 2008;25(1):30-39.
- Harkaeh S, Qari Y, Tashkandi H, et al. Thymoquinone nanoparticles protect against cisplatin-induced nephrotoxicity in Ehrlich carcinoma model without compromising cisplatin anticancer efficacy. *J King Saud University Sci*. 2022;34:101675.
- Dirican A, Sahin O, Tasli F, et al. Thymoquinone enhances cisplatin-induced nephrotoxicity in high dose. *J Oncol Sci*. 2016;1:17-24.
- Badary OA, Nagi MN, al-Shabanah OA, al-Sawaf HA, al-Sohaibani MO, al-Bekairi AM. Thymoquinone ameliorates the nephrotoxicity induced by cisplatin in rodents and potentiates its antitumor activity. *Can J Physiol Pharmacol*. 1997;75(12):1356-1361.
- Nessa MU, Beale P, Chan C, Yu JQ, Huq F. Synergism from combinations of cisplatin and oxaliplatin with quercetin and thymoquinone in human ovarian tumour models. *Anticancer Res*. 2011;31(11):3789-3797.
- Ulu R, Dogukan A, Tuzcu M, et al. Regulation of renal organic anion and cation transporters by thymoquinone in cisplatin induced kidney injury. *Food Chem Toxicol*. 2012;50(5):1675-1679.
- Farooqui Z, Shahid F, Khan AA, Khan F. Oral administration of Nigella sativa oil and thymoquinone attenuates long term cisplatin treatment induced toxicity and oxidative damage in rat kidney. *Biomed Pharmacother*. 2017;96:912-923.
- Al Fayi M, Otifi H, Alshyarba M, Dera AA, Rajagopalan P. Thymoquinone and curcumin combination protects cisplatin-induced kidney injury, nephrotoxicity by attenuating NFκB, KIM-1 and ameliorating Nrf2/HO-1 signalling. *J Drug Target*. 2020;28(9):913-922.
- El-Far AH, Tantawy MA, Al Jaouni SK, Mousa SA. Thymoquinone-chemotherapeutic combinations: new regimen to combat cancer and cancer stem cells. *Naunyn Schmiedebergs Arch Pharmacol*. 2020;393(9):1581-1598.
- Ganea GM, Fakayode SO, Losso JN, et al. Delivery of phytochemical thymoquinone using molecular micelle modified

- poly (D, L lactide-co-glycolide)(PLGA) nanoparticles. *Nanotechnology*. 2010;21:285104.
21. Elmowafy M, Samy A, Raslan MA, et al. Enhancement of bioavailability and pharmacodynamic effects of thymoquinone via nanostructured lipid carrier (NLC) formulation. *Aaps Pharmscitech*. 2016;17:663-672.
 22. Brigatte P, Sampaio SC, Gutierrez VP, et al. Walker 256 tumor-bearing rats as a model to study cancer pain. *J Pain*. 2007;8(5):412-421.
 23. Zhang Y, Fan Y, Huang S, et al. Thymoquinone inhibits the metastasis of renal cell cancer cells by inducing autophagy via AMPK/mTOR signaling pathway. *Cancer Sci*. 2018;109(12):3865-3873.
 24. Tang CH, Chen HL, Dong JR. Solid Lipid Nanoparticles (SLNs) and Nanostructured Lipid Carriers (NLCs) as food-grade nanovehicles for hydrophobic nutraceuticals or bioactives. *Appl Sci*. 2023;13:1726.
 25. Mahmoud YK, Abdelrazek HMA. Cancer: Thymoquinone antioxidant/pro-oxidant effect as potential anticancer remedy. *Biomed Pharmacother*. 2019;115:108783.
 26. Al-Shalabi E, Alkhalidi M, Sunoqrot S. Development and evaluation of polymeric nanocapsules for cirsiolol isolated from Jordanian *Teucrium polium* L. as a potential anticancer nanomedicine. *J Drug Deliv Sci Technol*. 2020;56:101544.
 27. Rice SB, Chan C, Brown SC, et al. Particle size distributions by transmission electron microscopy: an interlaboratory comparison case study. *Metrologia*. 2013;50(6):663-678. doi:10.1088/0026-1394/50/6/663.
 28. Feltin N, Crouzier L, Delvallée A, et al. Metrological protocols for reaching reliable and SI-traceable size results for multi-modal and complexly shaped reference nanoparticles. *Nanomaterials (Basel)*. 2023;9;13(6):993. doi:10.3390/nano13060993.
 29. Feczko T, Tóth J, Gyenis J. Comparison of the preparation of PLGA-BSA nano- and microparticles by PVA, poloxamer and PVP. *Colloids Surf*. 2008;319:188-195.
 30. Saghir SA, Al-Gabri NA, Khafaga AF, et al. Thymoquinone-PLGA-PVA nanoparticles ameliorate bleomycin-induced pulmonary fibrosis in rats via regulation of inflammatory cytokines and iNOS signaling. *Animals*. 2019;9:951.
 31. Vij N, Min T, Marasigan R, et al. Development of PEGylated PLGA nanoparticle for controlled and sustained drug delivery in cystic fibrosis. *J Nanobiotechnol*. 2010;8:22.
 32. UKCCCR. UKCCCR guidelines for the use of cell lines in cancer research. *Br J Cancer*. 2000;82:1495-1509.
 33. Feitosa IB, Mori B, Garcia Teles CB, et al. What are the immune responses during the growth of Ehrlich's tumor in ascitic and solid form? *Life Sci*. 2021;264:118578.
 34. Tousson E, Hafez E, Abo Gazia MM, Salem SB, Mutar TF. Hepatic ameliorative role of vitamin B17 against Ehrlich ascites carcinoma-induced liver toxicity. *Environ Sci Pollut Res Int*. 2020;27(9):9236-9246.
 35. Ali M, Mruthunjaya K, Nandini C, et al. Evaluation of beneficial effects of *Morinda citrifolia* L. in presence of cisplatin on Ehrlich's Ascites Carcinoma bearing mice. *Int J Pharm Sci Res*. 2018;9:305-312.
 36. Panesso MC, Shi M, Cho HJ, et al. Klotho has dual protective effects on cisplatin-induced acute kidney injury. *Kidney Int*. 2014;85:855-870. doi:10.1038/ki.2013.489.
 37. He Y, Chen X, Yu Z, et al. Sodium dicarboxylate cotransporter-1 expression in renal tissues and its role in rat experimental nephrolithiasis. *J Nephrol*. 2004;17:34-42.
 38. Abd Eldaim MA, Tousson E, El Sayed IET, Abd Elmaksoud AZ, Ahmed AAS. Ameliorative effects of 9-diaminoacridine derivative against Ehrlich ascites carcinoma-induced hepatorenal injury in mice. *Environ Sci Pollut Res Int*. 2021;28(17):21835-21850.
 39. Donia TI, Gerges MN, Mohamed TM. Amelioration effect of Egyptian sweet orange hesperidin on Ehrlich ascites carcinoma (EAC) bearing mice. *Chemico-biological Interactions*. 2018;285:76-84.
 40. Hashem MA, Shooeb SBA, Abd-Elhakim YM, et al. The antitumor activity of *Arthrospira platensis* and/or cisplatin in a murine model of Ehrlich ascites carcinoma with hematinic and hepatorenal protective action. *J Function Food*. 2020;66:103831.
 41. Adedara IA, Teberen R, Ebokaiwe AP, Ehwerhemuepha T, Farombi EO. Induction of oxidative stress in liver and kidney of rats exposed to Nigerian bonny light crude oil. *Environ Toxicol*. 2012;27(6):372-379.
 42. Yabuki A, Yoneshige S, Tanaka S, Tsujio M, Mitani S, Yamato O. Age-related histological changes in kidneys of Brown Norway rat. *J Vet Med Sci*. 2014;176(2): 277-280. doi:10.1292/jvms.13-0431.
 43. Al-Naimi MS, Rasheed HA, Hussien NR, Al- Kuraishy HM, Al-Gareeb AI. Nephrotoxicity: Role and significance of renal biomarkers in the early detection of acute renal injury. *J Adv Pharm Technol Res*. 2019;10(3):95-99. doi:10.4103/japtr. JAPTR_336_18.
 44. Chiou YY, Jiang ST, Ding YS, et al. Kidney-based in vivo model for drug-induced nephrotoxicity testing. *Sci Rep*. 2020;10:13640. <https://doi.org/10.1038/s41598-020-70502-3>.